

Different Mechanisms of Photochemical Re–Me and Re–Et Bond Homolysis in [Re(R)(CO)₃(4,4′-dimethyl-2,2′-bipyridine)]. A Time-Resolved IR Spectroscopic Study Ranging from Picoseconds to Microseconds[§]

Anders Gabrielsson,^{†,‡} Ana María Blanco-Rodríguez,[†] Pavel Matousek,[‡] Mike Towrie,[‡] and Antonín Vlček, Jr.*[‡]

School of Biological and Chemical Sciences, Queen Mary, University of London, Mile End Road, London E1 4NS, United Kingdom, and Central Laser Facility, CCLRC Rutherford Appleton Laboratory, Chilton, Didcot, Oxfordshire OX11 0QX, United Kingdom

Received October 15, 2005

The photochemistry of two metal-alkyl complexes, [Re(R)(CO)₃(dmb)] (R = methyl (Me), ethyl (Et)), was investigated by IR spectroscopy in the $\nu(\text{CO})$ spectral region, time-resolved over an exceptionally broad temporal range, from picoseconds to microseconds. Optical excitation of [Re(Et)(CO)₃(dmb)] in MeCN produces within the first two picoseconds the radicals [Re(MeCN)(CO)₃(dmb)][•] and Et[•], together with an excited state, which undergoes a slower (~90 ps) conversion to the same radicals. The reactive excited state was identified as ³MLCT (metal-to-ligand charge transfer) with an admixture of a ³SBLCT (sigma bond-to-ligand charge transfer) character. In CH₂Cl₂ solution, this excited state reacts with the solvent molecules to produce the radical anion [Re(Cl)(CO)₃(dmb)]^{•-} with ~130 ps kinetics. A series of slower reactions follows, forming [Re(CH₂Cl₂)(CO)₃(dmb)][•] and, ultimately, [Re(Cl)(CO)₃(dmb)]. The photochemical mechanism of [Re(Me)(CO)₃(dmb)] is different. Irradiation populates a ³MLCT excited state, which undergoes two parallel reactions: a thermally activated Re–Me bond homolysis and decay to the ground state. At room temperature, both reactions have the same time constant, ~34 ns, giving the photochemical quantum yield of about 0.5 and ³MLCT excited-state lifetime of 17 ns. The same reaction mechanism operates in CH₂Cl₂ and MeCN. The photoreactivity and excited-state behavior of both complexes are interpreted using qualitative potential energy surfaces. The striking difference between the ethyl and methyl complex is caused by different relative energies of the optically excited ¹MLCT state, the dissociative ³SBLCT state, and the ³MLCT state along the Re–R coordinate.

Introduction

Photochemical homolysis of metal–alkyl bonds is a convenient way to produce reactive alkyl and organometallic radicals.¹ Strongly colored alkyl- α -diimine and alkyl-polypyridine metal complexes can efficiently produce radicals even under irradiation with visible light. Such reactions have been observed for organometallic α -diimine complexes of Pt^{IV}, Pt^{II}, Ru^{II}, Re^I, and Mn^I or some main-group metals such as Zn^{II}.^{2–15} Irradiation of these complexes usually populates charge-transfer excited states

where the excited electron density is localized predominantly at the α -diimine ligand. An interesting question arises: how does such excitation trigger homolysis of a metal–alkyl bond? This was explained by invoking sigma bond-to-ligand charge-transfer (SBLCT, also called $\sigma\pi^*$) excited states, which involve excitation of electron density from a metal–alkyl σ -bonding orbital to a π^* orbital of the α -diimine ligand.^{16–27} Triplet ³SBLCT states are often unbound and correlate with radical

[§] This work is dedicated to the memory of Professor Derk J. Stufkens (Universiteit van Amsterdam), whose work has greatly advanced our understanding of spectroscopy, photochemistry, and photophysics of coordination compounds and inspired much further research, including the present study.

* To whom correspondence should be addressed. E-mail: a.vlcek@qmul.ac.uk.

[†] Queen Mary, University of London.

[‡] Current address: Institut für Anorganische Chemie der Universität Stuttgart, Pfaffenwaldring 55, D-70569, Stuttgart, Germany.

[§] CCLRC Rutherford Appleton Laboratory.

(1) Klingert, B.; Riediker, M.; Roloff, A. *Comments Inorg. Chem.* **1988**, *7*, 109–138.

(2) Kleverlaan, C. J.; Stufkens, D. J. *Inorg. Chim. Acta* **1999**, *284*, 61–70.

(3) Lucia, L. A.; Burton, R. D.; Schanze, K. S. *Inorg. Chim. Acta* **1993**, *208*, 103–106.

(4) Kleverlaan, C. J.; Stufkens, D. J.; Clark, I. P.; George, M. W.; Turner, J. J.; Martino, D. M.; van Willigen, H.; Vlček, A., Jr. *J. Am. Chem. Soc.* **1998**, *120*, 10871–10879.

(5) Farrell, I. R.; Matousek, P.; Kleverlaan, C. J.; Vlček, A., Jr. *Chem.-Eur. J.* **2000**, *6*, 1386–1394.

(6) Kleverlaan, C. J.; Martino, D. M.; van Willigen, H.; Stufkens, D. J.; Oskam, A. *J. Phys. Chem.* **1996**, *100*, 18607–18611.

(7) van Slageren, J.; Martino, D. M.; Kleverlaan, C. J.; Bussandri, A. P.; van Willigen, H.; Stufkens, D. J. *J. Phys. Chem. A* **2000**, *104*, 5969–5973.

(8) Kleverlaan, C. J.; Martino, D. M.; van Slageren, J.; van Willigen, H.; Stufkens, D. J.; Oskam, A. *Appl. Magn. Reson.* **1998**, *15*, 203–214.

(9) Rossenaar, B. D.; Stufkens, D. J.; Oskam, A.; Fraanje, J.; Goubitz, K. *Inorg. Chim. Acta* **1996**, *247*, 215–229.

(10) Kleverlaan, C. J.; Stufkens, D. J. *J. Photochem. Photobiol. A* **1998**, *116*, 109–118.

(11) Rossenaar, B. D.; Kleverlaan, C. J.; van de Ven, M. C. E.; Stufkens, D. J.; Vlček, A., Jr. *Chem. Eur. J.* **1996**, *2*, 228–237.

(12) Rossenaar, B. D.; Kleverlaan, C. J.; Stufkens, D. J.; Oskam, A. *J. Chem. Soc., Chem. Commun.* **1994**, 63–64.

(13) Hux, J. E.; Puddephatt, R. J. *J. Organomet. Chem.* **1992**, *437*, 251–263.

(14) Wissing, E.; Rijnberg, E.; van der Schaaf, P. A.; van Gorp, K.; Boersma, J.; van Koten, G. *Organometallics* **1994**, *13*, 2609–2615.

(15) Kaim, W.; Klein, A.; Hasenzahl, S.; Stoll, H.; Zálaiš, S.; Fiedler, J. *Organometallics* **1998**, *17*, 237–247.

(16) Stufkens, D. J.; Vlček, A., Jr. *The Spectrum* **1996**, *9* (2), 2–7.

(17) Stufkens, D. J.; Aarnts, M. P.; Rossenaar, B. D.; Vlček, A., Jr. *Pure Appl. Chem.* **1997**, *69*, 831–835.

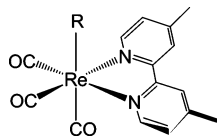


Figure 1. Schematic structure of the $[\text{Re}(\text{R})(\text{CO})_3(\text{dmb})]$ complexes, R = methyl (Me) or ethyl (Et).

products.^{26–29} SBLCT excited states are the only low-lying charge-transfer states in alkyl-diimine complexes of main-group metals or high-valence metals such as Pt^{IV} . The situation is more complicated in complexes of low-valence metals with low-lying metal-to-ligand charge-transfer excited states, MLCT. Their irradiation populates preferentially $^1\text{MLCT}$ states, and homolytic reactions are preceded by series of intersystem crossings and internal conversions between MLCT and SBLCT states.^{26,28,29} This is the case of $[\text{Re}(\text{R})(\text{CO})_3(\alpha\text{-diimine})]^{2-5,11,19}$ (R = alkyl, benzyl; see Figure 1) and analogous Mn^{II} complexes.

Photochemistry of $[\text{Re}(\text{R})(\text{CO})_3(\alpha\text{-diimine})]$ was found to depend strongly on the nature of the alkyl group, the α -diimine (2,2'-bipyridine vs bis-*i*-Pr-*N,N'*-1,4-diazabutadiene), and, for the diazabutadiene complexes, also the solvent.^{2–5,11,19} In particular, the photochemical reactivity of $[\text{Re}(\text{R})(\text{CO})_3(\text{dmb})]$ (dmb = 4,4'-dimethyl-2,2'-bipyridine) is strikingly different for R = methyl (Me) on one hand and R = ethyl (Et), isopropyl, or benzyl on the other.^{2,4,5,27} The methyl complex is emissive both at room temperature and in a 80 K glass.⁴ Irradiation into its MLCT absorption band leads to Re–Me homolysis, producing the radicals Me^{\bullet} and $[\text{Re}(\text{Solv})(\text{CO})_3(\text{dmb})]^{\bullet}$.^{2–4} Quantum yield of this reaction increases with increasing temperature, reaching the value of ca. 0.5 at room temperature.⁴ Nanosecond time-resolved IR (TRIR) spectra have provided evidence for population of a $^3\text{MLCT}$ state and independent radical formation.⁴ The same conclusion was drawn from time-resolved visible absorption experiments, TR–vis, measured in the hundreds of femtoseconds to nanoseconds time-domain.^{4,5} Decay of the emission and excited-state absorption provided the value of ~ 30 ns for the $^3\text{MLCT}$ lifetime in THF, at room temperature.⁴ FT-EPR spectroscopy has shown that Me^{\bullet} radicals are formed within the 50 ns instrument time resolution from a spin-triplet precursor. These results were interpreted as evidence for an ultrafast Re–Me bond homolysis that is competitive with relaxation to an unreactive $^3\text{MLCT}$ state.^{4,5,30} On the other hand, the quantum yield of Re–R homolysis in the analogous complexes $[\text{Re}(\text{R})(\text{CO})_3(\text{dmb})]$ (R = Et, isopropyl, benzyl) is unity, regardless of the temperature.⁴ FT-EPR again indicates a spin-triplet precursor for the formation of the organic radicals R^{\bullet} .^{4,6,8} Kinetic analysis

of picosecond TR–vis spectra of the ethyl complex indicated that the solvated radicals $[\text{Re}(\text{Solv})(\text{CO})_3(\text{dmb})]^{\bullet}$ are formed via two pathways: a prompt one, completed in ≤ 800 fs, and a delayed reaction via a $^3\text{MLCT}$ state, for which a time constant of ca. 83 ps was determined in MeCN.⁵

Most of the previous mechanistic conclusions were inferred from quantum yield measurements and TR–vis spectra, which are not structure-sensitive enough to distinguish and identify the excited states and intermediates involved. Herein, we compare the photochemistry of $[\text{Re}(\text{Me})(\text{CO})_3(\text{dmb})]$ and $[\text{Re}(\text{Et})(\text{CO})_3(\text{dmb})]$ (Figure 1) studied by time-resolved IR spectroscopy over a temporal range spanning from units of picoseconds to hundreds of microseconds, aiming at (i) direct observation and characterization of the reactive excited state(s), (ii) determination of the rates of Re–Me and Re–Et excited-state homolysis, (iii) understanding the striking differences in the photoreactivity of Et and Me complexes, and (iv) comparing the photoreactivity in CH_3CN and CH_2Cl_2 . The Re–alkyl bond homolysis from a $^3\text{MLCT}$ state is documented for the first time, and a new photochemical mechanism is proposed for the methyl complex. Unexpectedly, the excited ethyl and methyl complex were found to differ in their reactivity toward CH_2Cl_2 , whereby electron transfer prevails over Re–C bond dissociation for Et, but not Me. The spectroscopic data allow us to explain the photochemistry of both complexes and the dependence on the nature of the alkyl ligand. These results could have more general implications for photochemistry of transition-metal alkyl complexes.

Experimental Section

Materials. The $[\text{Re}(\text{R})(\text{CO})_3(\text{dmb})]$ complexes were prepared following a modified literature procedure.^{3,4} $[\text{Re}(\text{Cl})(\text{CO})_3(\text{dmb})]$ was suspended in THF (50 mL) and cooled on ice. Then 1.1 equiv of the Grignard reagent (3 M solution of CH_3MgCl or $\text{C}_2\text{H}_5\text{MgCl}$ in THF) was added dropwise by a syringe. The progress of the substitution was monitored by FTIR, and the reaction was quenched by adding 1 mL of water (degassed) when the starting material had disappeared. The solvent was then removed in vacuo. CH_2Cl_2 was added, and the solid magnesium salts were removed by filtration. The solvent was removed to give a yellow solid. IR and ^1H NMR spectra of the product were identical to the published ones.²

Spectroscopic studies were carried out in MeCN or CH_2Cl_2 of spectroscopic grade (Aldrich).

Time-Resolved IR Spectroscopy (TRIR). Time-resolved IR measurements used the equipment and procedures described in detail previously.^{31,32} In short, the sample solution was excited (pumped) at 400 nm, using frequency-doubled pulses from a Ti:sapphire laser of ~ 150 fs duration (fwhm) and ~ 3 μJ energy, focused at an area of ca. 200 μJ diameter. Sum-frequency generation was used to pump at 355 nm, combining the 800 nm fundamental with OPA-produced 638 nm light. TRIR spectra were probed with IR (~ 150 fs) pulses obtained by difference-frequency generation. The IR probe pulses cover a spectral range ~ 200 cm^{-1} wide. The sample solutions were flowed through a 0.1–0.5 mm CaF_2 IR cell, which was rastering in two dimensions. Kinetic fitting was performed using Microcal Origin 7 software. The spectra are shown from 2 ps onward, when the early coherence effects have subsided. The same instrument was used to measure TRIR spectra in the nanosecond range. The sample was excited with ~ 1 ns, 355 nm

(18) Stufkens, D. J.; Aarnts, M. P.; Nijhoff, J.; Rossenaar, B. D.; Vlček, A., Jr. *Coord. Chem. Rev.* **1998**, *171*, 93–105.

(19) Rossenaar, B. D.; George, M. W.; Johnson, F. P. A.; Stufkens, D. J.; Turner, J. J.; Vlček, A., Jr. *J. Am. Chem. Soc.* **1995**, *117*, 11582–11583.

(20) Aarnts, M. P.; Stufkens, D. J.; Wilms, M. P.; Baerends, E. J.; Vlček, A., Jr.; Clark, I. P.; George, M. W.; Turner, J. J. *Chem. Eur. J.* **1996**, *2*, 1556–1565.

(21) Rossenaar, B. D.; Lindsay, E.; Stufkens, D. J.; Vlček, A., Jr. *Inorg. Chim. Acta* **1996**, *250*, 5–14.

(22) Stufkens, D. J.; Vlček, A., Jr. *Coord. Chem. Rev.* **1998**, *177*, 127–179.

(23) Daniel, C. *Coord. Chem. Rev.* **2002**, *230*, 65–78.

(24) Turki, M.; Daniel, C. *Coord. Chem. Rev.* **2001**, *216–217*, 31–43.

(25) Turki, M.; Daniel, C.; Zálaiš, S.; Vlček, A., Jr.; van Slageren, J.; Stufkens, D. J. *J. Am. Chem. Soc.* **2001**, *123*, 11431–11440.

(26) Bruand-Cote, I.; Daniel, C. *Chem. Eur. J.* **2002**, *8*, 1361–1183.

(27) Guillaumont, D.; Wilms, M. P.; Daniel, C.; Stufkens, D. J. *Inorg. Chem.* **1998**, *37*, 5816.

(28) Finger, K.; Daniel, C. *J. Am. Chem. Soc.* **1995**, *117*, 12322–12327.

(29) Guillaumont, D.; Daniel, C. *J. Am. Chem. Soc.* **1999**, *121*, 11733–11743.

(30) Vlček, A., Jr. *Coord. Chem. Rev.* **1998**, *177*, 219–256.

(31) Towrie, M.; Grills, D. C.; Dyer, J.; Weinstein, J. A.; Matousek, P.; Barton, R.; Bailey, P. D.; Subramaniam, N.; Kwok, W. M.; Ma, C. S.; Phillips, D.; Parker, A. W.; George, M. W. *Appl. Spectrosc.* **2003**, *57*, 367–380.

(32) Vlček, A., Jr.; Farrell, I. R.; Liard, D. J.; Matousek, P.; Towrie, M.; Parker, A. W.; Grills, D. C.; George, M. W. *J. Chem. Soc., Dalton Trans.* **2002**, 701–712.

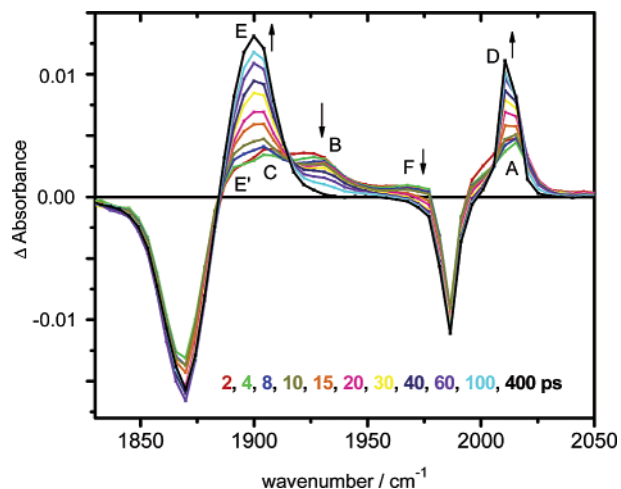


Figure 2. Difference time-resolved IR spectra of $[\text{Re}(\text{Et})(\text{CO})_3\text{-(dmb)}]$ in MeCN measured at selected time delays after ~ 150 fs, 400 nm laser pulse excitation. Experimental points are separated by 4–5 cm^{-1} . Assignment of IR bands: ${}^3\text{MLCT}$: A, B, C; $[\text{Re}(\text{Et})(\text{CO})_3(\text{dmb})]^*$: D, E.

pulses and probed with ~ 150 fs, 200 cm^{-1} broad IR pulses generated as described above. The nanosecond pump laser and the femtosecond IR spectrometer were synchronized electronically.³³

Results

$[\text{Re}(\text{Et})(\text{CO})_3(\text{dmb})]$. Figure 2 shows the picosecond time-resolved IR spectra of $[\text{Re}(\text{Et})(\text{CO})_3(\text{dmb})]$ measured in MeCN

after 400 nm excitation. The spectra obtained at shortest time delays (2–4 ps) exhibit negative bleach bands at 1987 and ~ 1867 cm^{-1} , due to the depletion of the ground-state population, together with positive bands at 2015 (A), 1926–1931 (B), and 1905 (C) cm^{-1} and a shoulder at 1890–1895 cm^{-1} (E'). In addition, there is a broad feature F, which extends over most of the spectrum. It is clearly visible between 1960 and 1976 cm^{-1} , overlapping with the 1987 cm^{-1} bleach. The growing bands D and E occur at 2011 and 1895–1900 cm^{-1} , respectively. At early time delays, they overlap with the features A and C, respectively.

The growth of the bands D and E is biexponential with the time constants of 20 ± 4 and 92 ± 21 ps, whose amplitude ratio is ca. 1.75:1. The band B (1926–1931 cm^{-1}) decays with a time constant of 89 ± 14 ps, which is comparable to the longer rise component. The conversion from B to E is nearly isobestic. The broad feature F decays with a ca. 22 ps lifetime, as measured at 1972 cm^{-1} . The bleach bands do not show any recovery throughout the time interval investigated.

The characteristic^{34–42} IR pattern of the bands A, B, and C (2015, 1926–1931, 1905 cm^{-1} , respectively) warrants their assignment to a ${}^3\text{MLCT}$ excited state. The growing product bands D and E (2011, 1895–1900 cm^{-1} , respectively) are attributed to the solvated radical $[\text{Re}(\text{CH}_3\text{CN})(\text{CO})_3(\text{dmb})]^*$ by comparison with the IR spectrum of electrochemically generated $[\text{Re}(\text{CH}_3\text{CN})(\text{CO})_3(\text{bpy})]^*$, which is characterized⁴³ by bands at 2011 and 1895 cm^{-1} (broad). The feature F is very broad, indicating that it belongs to a vibrationally hot species, which can be a partly dissociated ${}^3\text{SBLCT}$ state, a radical pair, or,

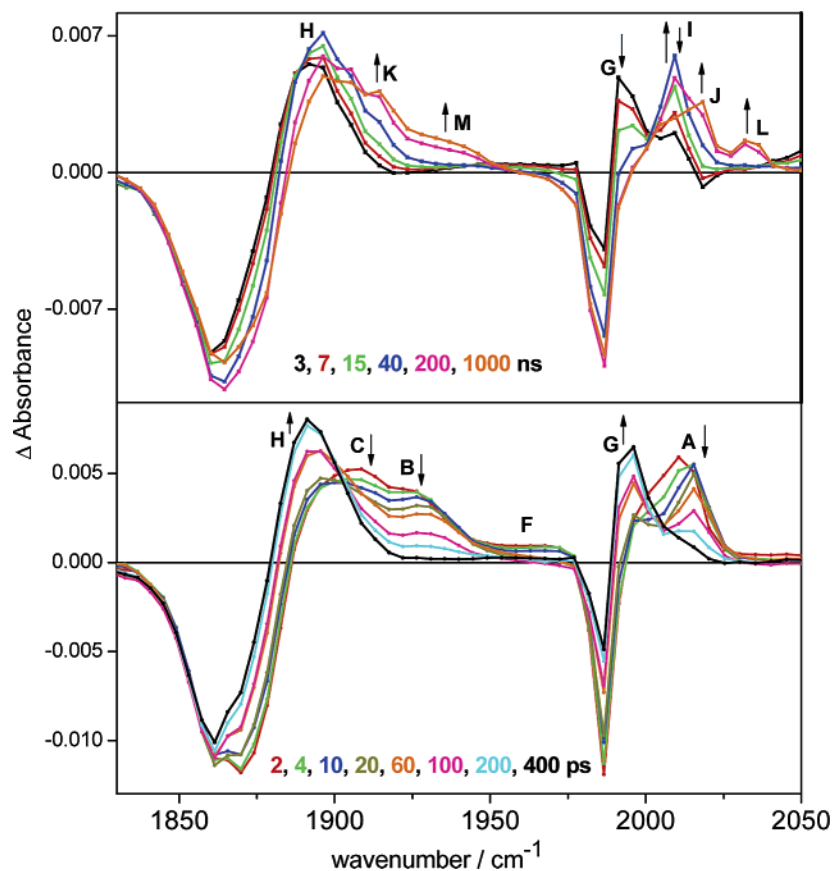


Figure 3. Difference time-resolved IR spectra of $[\text{Re}(\text{Et})(\text{CO})_3(\text{dmb})]$ in CH_2Cl_2 measured at selected time delays after laser pulse excitation. Experimental points are separated by 4–5 cm^{-1} . Bottom: picosecond spectra, excited at 400 nm. Top: nanosecond spectra measured from an air-saturated solution, excited at 355 nm. Assignment of IR bands: ${}^3\text{MLCT}$: A, B, C; $[\text{Re}(\text{Cl})(\text{CO})_3(\text{dmb})]^-$: G, H; $[\text{Re}(\text{CH}_2\text{Cl}_2)(\text{CO})_3(\text{dmb})]^*$: I; $[\text{Re}(\text{Cl})(\text{CO})_3(\text{dmb})]$: J, K; $[\text{Re}(\text{CH}_2\text{Cl}_2)(\text{CO})_3(\text{dmb})]^+$: L, M.

most likely, an unequilibrated radical product $^{\#}[\text{Re}(\dots\text{CH}_3\text{CN})(\text{CO})_3(\text{bpy})]^{\bullet}$.

Spectra measured using 355 nm excitation show the same features and dynamics, although their quantitative analysis is prevented by a much lower signal-to-noise ratio.

The photochemistry of $[\text{Re}(\text{Et})(\text{CO})_3(\text{dmb})]$ changes profoundly on going to CH_2Cl_2 ; see Figure 3. The spectra measured immediately after excitation (2–4 ps) are very similar to those taken in MeCN. They show bleach bands at 1987 and 1870 cm^{-1} , $^3\text{MLCT}$ transient bands at 2016 (A), 1926 (B), and 1906 (C) cm^{-1} , and the weak, very broad absorption F at 1950–1975 cm^{-1} . The bands A, B, and C decay with a time constant estimated as 127 ps to form two product bands at 1996 (G) and ~ 1891 cm^{-1} (H). The band H strongly overlaps with the bleach and should better be described as 1885–1891 cm^{-1} . These spectral features are clearly different from those of $[\text{Re}(\text{CH}_2\text{Cl}_2)(\text{CO})_3(\text{dmb})]^{\bullet}$, obtained after photolysis of $[\text{Re}(\text{Me})(\text{CO})_3(\text{dmb})]$ in CH_2Cl_2 ; see Figure 5. Instead, the product spectrum closely resembles that of $[\text{Re}(\text{Cl})(\text{CO})_3(\text{bpy})]^{\bullet}$ electrochemically generated in THF in the presence of excess $[(n\text{-Bu})_4\text{N}]\text{Cl}$, which is characterized by bands at 1996 and 1868–1883 cm^{-1} .^{43,44} The photoproduct is thus assigned as a radical anion $[\text{Re}(\text{Cl})(\text{CO})_3(\text{dmb})]^{\bullet-}$. The corresponding bands G and H grow with kinetics commensurate with those of the $^3\text{MLCT}$ decay, confirming a direct conversion of the $^3\text{MLCT}$ state of $[\text{Re}(\text{Et})(\text{CO})_3(\text{dmb})]$ into $[\text{Re}(\text{Cl})(\text{CO})_3(\text{dmb})]^{\bullet-}$. (The rise of the product bands seems to contain a minor, faster component, which could be caused by a reaction of the hot species. However, a strong band overlap and simultaneous decay of the broad feature F, which is completed in ~ 30 ps, prevent detailed kinetic analysis.)

On a nanosecond time scale, the band G (1996 cm^{-1}) decays and a new band I at 2011 cm^{-1} rises isospectically. The product is assigned as $[\text{Re}(\text{CH}_2\text{Cl}_2)(\text{CO})_3(\text{dmb})]^{\bullet}$, since the band I is identical with that of the photolysis product of $[\text{Re}(\text{Me})(\text{CO})_3(\text{dmb})]$ in CH_2Cl_2 (vide infra) and closely resembles the IR band of $[\text{Re}(\text{MeCN})(\text{CO})_3(\text{dmb})]^{\bullet}$. A time constant of ca. 24 ns was determined for this conversion from the decay and rise of the bands G and I, respectively. On a longer time scale (50–500 ns), the $[\text{Re}(\text{CH}_2\text{Cl}_2)(\text{CO})_3(\text{dmb})]^{\bullet}$ band I decays, being replaced by bands J and K at ~ 2020 and ~ 1915 cm^{-1} . These features stay constant until the end of the time interval investigated, that is, 2 μs . They correspond to $[\text{Re}(\text{Cl})(\text{CO})_3(\text{dmb})]$, whose authentic sample is characterized by $\nu(\text{CO})$ bands at 2022, 1918, and 1895 cm^{-1} in CH_2Cl_2 . In addition, a small byproduct peak L at 2034 cm^{-1} was observed growing in the spectra measured

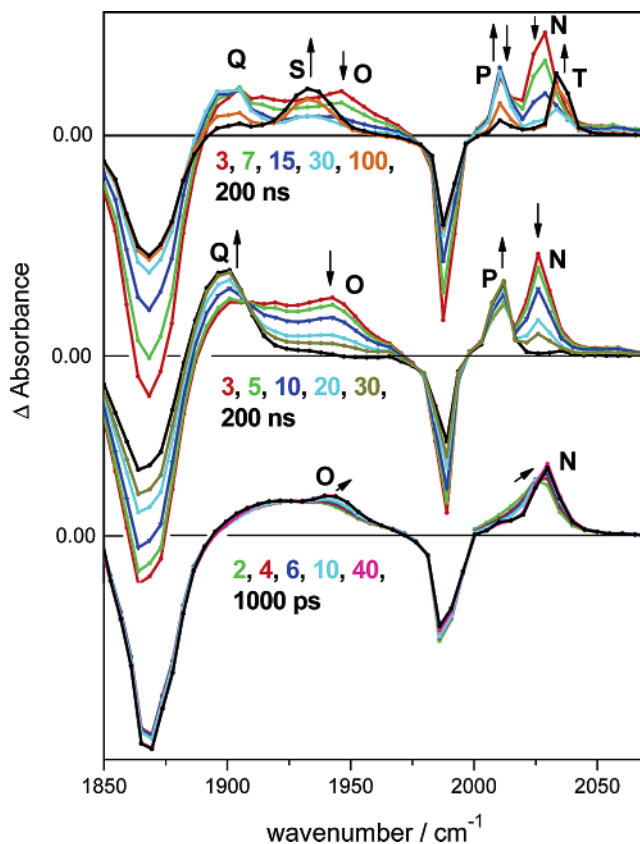


Figure 4. Difference time-resolved IR spectra of $[\text{Re}(\text{Me})(\text{CO})_3(\text{dmb})]$ in MeCN measured at selected time delays after laser pulse excitation. Spectral evolution is indicated by arrows. Experimental points are separated by 4–5 cm^{-1} . Bottom: picosecond spectra. Middle: nanosecond spectra, degassed solution. Top: nanosecond spectra, air-saturated solution. Assignment of IR bands: $^3\text{MLCT}$: N, O; $[\text{Re}(\text{MeCN})(\text{CO})_3(\text{dmb})]^{\bullet}$: P, Q; $[\text{Re}(\text{MeCN})(\text{CO})_3(\text{dmb})]^{\bullet+}$: T, S.

at time delays longer than 200 ns. This is a typical wavenumber for cationic Re(I) complexes. Hence, it is tentatively assigned as $[\text{Re}(\text{CH}_2\text{Cl}_2)(\text{CO})_3(\text{dmb})]^{\bullet+}$, formed by oxidation of the radical by air. It also contributes to the slowly growing absorption M at ~ 1935 cm^{-1} .

$[\text{Re}(\text{Me})(\text{CO})_3(\text{dmb})]$. Time-resolved IR spectra of $[\text{Re}(\text{Me})(\text{CO})_3(\text{dmb})]$ in MeCN measured from 2 to 1000 ps after 400 nm excitation (Figure 4) show two negative bleach bands at 1987 and 1867 cm^{-1} , due to depletion of the ground-state population, a sharp positive band N at 2030 cm^{-1} , and a broad absorption feature O between 1900 and 1960 cm^{-1} that appears to encompass two bands. This pattern is characteristic^{34–42} of a $^3\text{MLCT}$ excited state as seen, for example, for $[\text{Re}(\text{Cl})(\text{CO})_3(\text{bpy})]$ or $[\text{Re}(\text{Etpy})(\text{CO})_3(\text{dmb})]^{\bullet+}$. The $^3\text{MLCT}$ state is initially formed vibrationally hot. This is manifested by larger widths and lower wavenumbers of the bands in the spectra measured immediately after excitation. The small narrowing and upward shift seen in the ps TRIR spectrum (Figure 4) can be attributed to vibrational cooling, which includes solvent relaxation.^{41,45} On a nanosecond time scale (Figure 4, middle, top), the $^3\text{MLCT}$ band N (2030 cm^{-1}) decays with lifetimes of 12 ± 0.4 and 17 ± 0.3 ns in air-saturated and degassed solutions, respectively. A very similar lifetime (16 ± 0.5 ns) was determined in a degassed solution for the decay of the lower $^3\text{MLCT}$ band O. The $^3\text{MLCT}$ decay is accompanied by growth of bands at 2011

(33) Towrie, M.; Parker, A. W.; Vlček, A., Jr.; Gabrielsson, A.; Blanco Rodriguez, A. M. *Appl. Spectrosc.* **2005**, *59*, 467–473.

(34) Glyn, P.; George, M. W.; Hodges, P. M.; Turner, J. J. *J. Chem. Soc., Chem. Commun.* **1989**, 1655–1657.

(35) George, M. W.; Johnson, F. P. A.; Westwell, J. R.; Hodges, P. M.; Turner, J. J. *J. Chem. Soc., Dalton Trans.* **1993**, 2977–2979.

(36) Gamelin, D. R.; George, M. W.; Glyn, P.; Grevels, F.-W.; Johnson, F. P. A.; Klotzbücher, W.; Morrison, S. L.; Russell, G.; Schaffner, K.; Turner, J. J. *Inorg. Chem.* **1994**, *33*, 3246–3250.

(37) Bignozzi, C. A.; Schoonover, J. R.; Dyer, R. B. *Comments Inorg. Chem.* **1996**, *18*, 77–100.

(38) Schoonover, J. R.; Strouse, G. F.; Omberg, K. M.; Dyer, R. B. *Comments Inorg. Chem.* **1996**, *18*, 165–188.

(39) Schoonover, J. R.; Strouse, G. F. *Chem. Rev.* **1998**, *98*, 1335–1355.

(40) Dattelbaum, D. M.; Omberg, K. M.; Schoonover, J. R.; Martin, R. L.; Meyer, T. J. *Inorg. Chem.* **2002**, *41*, 6071–6079.

(41) Liard, D. J.; Busby, M.; Matousek, P.; Towrie, M.; Vlček, A., Jr. *J. Phys. Chem. A* **2004**, *108*, 2363–2369.

(42) Busby, M.; Matousek, P.; Towrie, M.; Clark, I. P.; Motevalli, M.; Hartl, F.; Vlček, A., Jr. *Inorg. Chem.* **2004**, *43*, 4523–4530.

(43) Johnson, F. P. A.; George, M. W.; Hartl, F.; Turner, J. J. *Organometallics* **1996**, *15*, 3374–3387.

(44) Stor, G. J.; Hartl, F.; van Outersterp, J. W. M.; Stufkens, D. J. *Organometallics* **1995**, *14*, 1115–1131.

(45) Asbury, J. B.; Wang, Y.; Lian, T. *Bull. Chem. Soc. Jpn.* **2002**, *75*, 973–983.

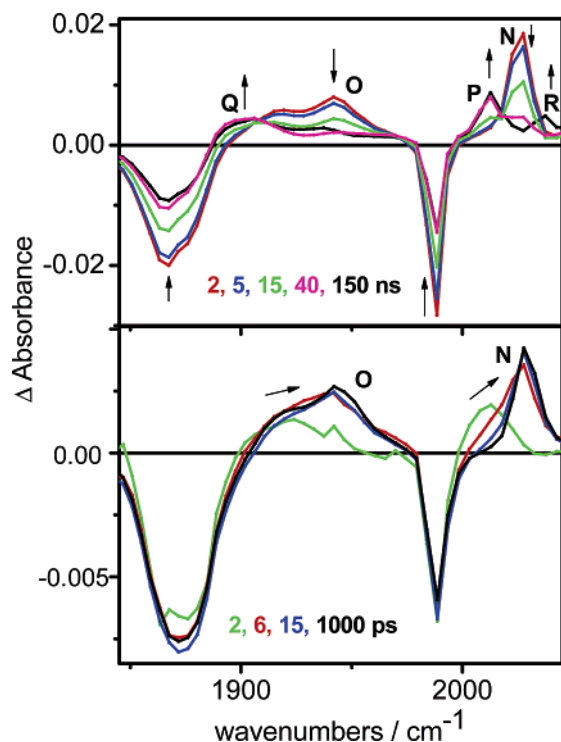


Figure 5. Difference time-resolved IR spectra of $[\text{Re}(\text{Me})(\text{CO})_3(\text{dmb})]$ in air-saturated CH_2Cl_2 . Bottom: Picosecond spectra measured at selected time delays after 400 nm, ~ 150 fs laser pulse excitation. Top: Nanosecond spectra measured at selected time delays after 355 nm, ~ 1 ns laser pulse excitation. Spectral evolution is indicated by arrows. Experimental points are separated by 4–5 cm^{-1} . Assignment of IR bands: ${}^3\text{MLCT}$: N, O; $[\text{Re}(\text{CH}_2\text{Cl}_2)(\text{CO})_3(\text{dmb})]^*$: P, Q; $[\text{Re}(\text{CH}_2\text{Cl}_2)(\text{CO})_3(\text{dmb})]^+$: R.

(P) and ~ 1900 cm^{-1} (Q) due to $[\text{Re}(\text{CH}_3\text{CN})(\text{CO})_3(\text{dmb})]^*$ (this assignment is based on comparison with the TRIR spectra of $[\text{Re}(\text{Et})(\text{CO})_3(\text{dmb})]$ in MeCN, Figure 2, and of the electrochemically generated⁴³ $[\text{Re}(\text{CH}_3\text{CN})(\text{CO})_3(\text{bpy})]^*$). Time constants of 10 ± 2 and 20 ± 6 ns were measured for the growth of the 2011 cm^{-1} radical band P, in air-saturated and degassed solutions, respectively. Approximately 50% of the ground state recovers with kinetics equal to those of the ${}^3\text{MLCT}$ decay and the radical formation. This is manifested by the $\sim 50\%$ decay of both bleach bands, for which lifetimes of 17 ± 0.6 and 18 ± 0.6 ns were determined at 1987 and 1867 cm^{-1} , respectively, in a degassed solution. It follows that the ${}^3\text{MLCT}$ state simultaneously decays to the ground state and reacts to the radicals, with an apparent time constant of ~ 17 ns. The 50% bleach recovery indicates that the radicals are formed with a quantum yield of about 0.5. The radical bands decay only very slowly in a deoxygenated solution, after the maximum intensity is reached at ca. 50 ns. Oxidation of the radical to a cationic product $[\text{Re}(\text{CH}_3\text{CN})(\text{CO})_3(\text{dmb})]^+$, characterized by the bands T and S at 2034 and 1932 cm^{-1} , respectively, occurs in air-saturated solutions. The maximum radical signal is reached at 15–20 ns, followed by a 83 ± 13 ns decay. The growing bands of $[\text{Re}(\text{CH}_3\text{CN})(\text{CO})_3(\text{dmb})]^+$ become apparent at 100 ns and later.

Time-resolved IR spectra of $[\text{Re}(\text{Me})(\text{CO})_3(\text{dmb})]$ measured in CH_2Cl_2 from 2 ps to 150 ns are shown in Figure 5. Picosecond spectra show only bleached ground-state bands at 1872 and 1989 cm^{-1} , together with the features at 2028 (N) and 1910–1960 cm^{-1} (O) that belong to a ${}^3\text{MLCT}$ excited state. In the nanosecond range, the ${}^3\text{MLCT}$ bands decay completely, while the bleach recovers by about 50% and product bands at 2012

(P) and ~ 1902 cm^{-1} (Q) grow in. The conversion is isosbestic, and the time constants of all three processes are identical within the experimental accuracy: 17 ± 1.2 , 19 ± 0.2 , and 24 ± 4 ns for the bleach recovery at 1989 cm^{-1} , ${}^3\text{MLCT}$ decay at 2027 cm^{-1} , and product formation at 2012 cm^{-1} , respectively. The product bands are attributed to the solvated radical $[\text{Re}(\text{CH}_2\text{Cl}_2)(\text{CO})_3(\text{dmb})]^*$, because of their similarity with the spectrum of $[\text{Re}(\text{CH}_2\text{Cl}_2)(\text{CO})_3(\text{dmb})]^*$, generated photochemically from the ethyl complex in CH_2Cl_2 (Figure 3) and of the electrochemically produced⁴³ $[\text{Re}(\text{MeCN})(\text{CO})_3(\text{bpy})]^*$. The bleach recovery indicates that the quantum yield of the radical formation is about 0.5. This value agrees with that determined in toluene under stationary 488 nm irradiation: 0.42 at 293 K.⁴ On a still longer time scale, between 150 ns and 10 μs (not shown in Figure 5), the spectrum of the radical converts to that of $[\text{Re}(\text{Cl})(\text{CO})_3(\text{dmb})]$, characterized by bands at ~ 2019 and 1894–1920 (br) cm^{-1} . A time constant of 1.4 μs has been estimated previously⁴⁶ for this reaction. A small amount of the oxidation product, $[\text{Re}(\text{CH}_2\text{Cl}_2)(\text{CO})_3(\text{dmb})]^+$, is formed in air-saturated solution, characterized by the band R (~ 2034 cm^{-1}).

Discussion

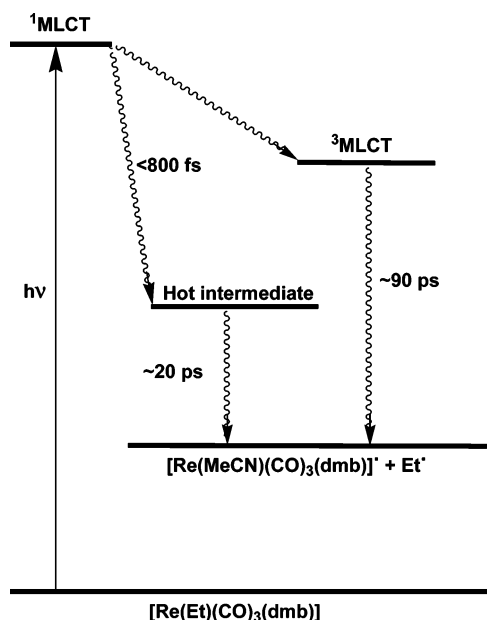
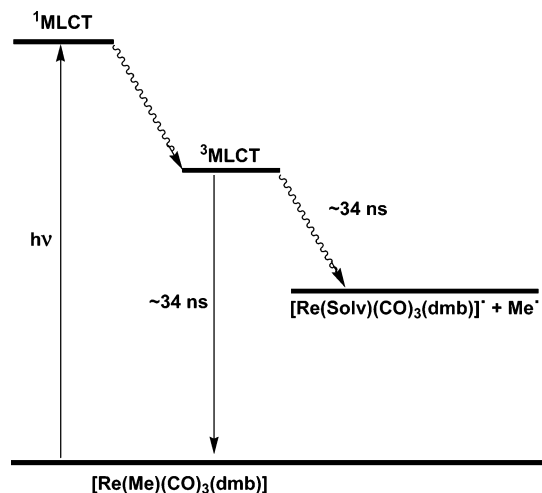
Excited-State Characters. Near-UV (400 or 355 nm) irradiation of either $[\text{Re}(\text{R})(\text{CO})_3(\text{dmb})]$ complex (R = Et, Me) leads to population of an excited-state whose $\nu(\text{CO})$ IR spectral pattern is characteristic of a ${}^3\text{MLCT}$ state, whereby the bands occur at higher wavenumbers than in the ground state.^{34–42} The upward shifts of A, B, and C bands of $[\text{Re}(\text{Et})(\text{CO})_3(\text{dmb})]$ (+28, +62, +38 cm^{-1} , respectively, in MeCN) are smaller than seen for $[\text{Re}(\text{Me})(\text{CO})_3(\text{dmb})]$ (+43, ca. +74, ca. +53 cm^{-1} in MeCN). The latter shift values are well comparable to those seen for the corresponding bands of complexes with typical ${}^3\text{MLCT}$ lowest excited states, such as $[\text{Re}(\text{Cl})(\text{CO})_3(\text{bpy})]$ (+40, +66, +58 cm^{-1} in CH_2Cl_2)³⁵ or $[\text{Re}(4\text{-Et-py})(\text{CO})_3(\text{dmb})]^+$ (+37, +81, +33 cm^{-1} in MeCN).^{41,47} The smaller shift of the band A in the case of $[\text{Re}(\text{Et})(\text{CO})_3(\text{dmb})]$ indicates an admixture of a ${}^3\text{SBLCT}$ character into the ${}^3\text{MLCT}$ state, whereby part of the excited electron energy originates in the Et[−] ligand or a Re–Et σ bond. However, considering that pure ${}^3\text{SBLCT}$ excited-state character manifests itself by a small negative shift of the highest $\nu(\text{CO})$ band,¹⁹ we may conclude that the observed excited state of $[\text{Re}(\text{Et})(\text{CO})_3(\text{dmb})]$ is still predominantly ${}^3\text{MLCT}$ in character.

Excited-State Dynamics and Mechanisms of Re–R Homolysis. The photochemical mechanisms of $[\text{Re}(\text{Et})(\text{CO})_3(\text{dmb})]$ in MeCN and $[\text{Re}(\text{Me})(\text{CO})_3(\text{dmb})]$ in MeCN or CH_2Cl_2 , deduced from the TRIR spectra, are summarized in Schemes 1 and 2, while the corresponding qualitative potential energy curves are shown in Scheme 3. Table 1 summarizes $\nu(\text{CO})$ wavenumbers of all the species studied herein. Near-UV (400 or 355 nm) of either complex produces^{2,4} the ${}^1\text{MLCT}$ state, but the subsequent dynamics are very different for the Me and Et complex, and, for the latter, for the solvent.

For $[\text{Re}(\text{Et})(\text{CO})_3(\text{dmb})]$, optical excitation is followed by a simultaneous subpicosecond formation of the unequilibrated $^{\#}[\text{Re}(\dots\text{CH}_3\text{CN})(\text{CO})_3(\text{dmb})]^*$ radical and intersystem crossing to the ${}^3\text{MLCT}$ state; see Scheme 1. The IR absorption of the hot radical consists of the very broad feature F and the shoulder E', and, possibly, it also contributes to the initial broadening of the band A (Figure 2). Equilibration, that is, vibrational cooling

(46) Clark, I. P. Time-resolved infrared spectroscopy of organometallic excited states. Ph.D. Thesis, University of Nottingham, Nottingham, 1997.

(47) Dattelbaum, D. M.; Martin, R. L.; Schoonover, J. R.; Meyer, T. J. *J. Phys. Chem. A* **2004**, *108*, 3518–3526.

Scheme 1. Photochemistry of $[\text{Re}(\text{Et})(\text{CO})_3(\text{dmb})]$ in MeCNScheme 2. Photochemistry of $[\text{Re}(\text{Me})(\text{CO})_3(\text{dmb})]^a$ 

^a Solv = MeCN or CH_2Cl_2 .

of the hot radical and its full solvation, occurs with a 20 ps kinetics seen as the decay of F and the faster component of the rise of the bands D and E due to the $[\text{Re}(\text{CH}_3\text{CN})(\text{CO})_3(\text{dmb})]^*$ product. Similar picosecond growth of photoproduct bands from a very broad IR absorption has been seen before for CO-loss photoproducts, radicals, or triplet states formed upon laser-pulse excitation of various metal-carbonyls.^{48–54} (In fact, we cannot fully assess the extent of the Re–Et bond breaking in the hot

intermediate. It cannot be excluded that the broad features F and E' belong to a $^3\text{SBLCT}$ state with elongated Re–Et bond or a radical pair.) The intersystem crossing to the $^3\text{MLCT}$ state is manifested by the “immediate” appearance of the IR features A, B, and C, Figure 2. The $^3\text{MLCT}$ state undergoes a ~ 90 ps Re–Et bond homolysis, producing the thermally equilibrated solvated radical $[\text{Re}(\text{CH}_3\text{CN})(\text{CO})_3(\text{dmb})]^*$. This process is manifested by the isosbestic conversion of the feature B to E, the ~ 90 ps kinetics of the decay of B, and the slower (~ 90 ps) kinetic component of the rise of the bands D and E. This reaction presumably proceeds via a lower lying unbound $^3\text{SBLCT}$ state.

The mechanism proposed herein from the TRIR spectra agrees with that inferred earlier from TR–vis spectra,⁵ where it was concluded that the Re–Et homolysis follows two pathways: (i) a “prompt” one, which originates in the optically populated $^1\text{MLCT}$ state and involves intersystem crossing onto the dissociative $^3\text{SBLCT}$ surface, and (ii) a delayed reaction that proceeds through the $^3\text{MLCT}$ state. The time constants of the prompt and “delayed” radical formation determined herein by TRIR, $\ll 2$ ps and ~ 90 ps, agree well with those measured by TR–vis,⁵ ~ 800 fs and 83 ps, respectively.

The excited-state behavior of $[\text{Re}(\text{Me})(\text{CO})_3(\text{dmb})]$ (Scheme 2) is very different from its Et counterpart: the prompt reaction is absent, while the “delayed” pathway is much slower and, as shown before,⁴ thermally activated. The only transient observed by TRIR on a picosecond time scale is the $^3\text{MLCT}$ state, characterized by the bands N and O, Figures 4 and 5. The $^3\text{MLCT}$ excited-state population decays simultaneously to the ground state and to $[\text{Re}(\text{Solv})(\text{CO})_3(\text{dmb})]^*$ radicals, manifested by the bands P and Q, Figures 4 and 5. The concomitantly produced Me^* radicals were detected independently by FT-EPR.^{4,5,30} The $^3\text{MLCT}$ lifetime of 17 ns and a photochemical quantum yield of ca. 0.5 were determined from the TRIR spectra. From these values, it follows that the time constants of Re–Me homolysis and decay to the ground state are comparable, ca. 34 ns. The quantum yield determined by TRIR on the nanosecond time scale is identical to that measured using stationary irradiation.^{2,4} This shows that the nanosecond branching of the $^3\text{MLCT}$ state evolution determines the overall photochemistry of $[\text{Re}(\text{Me})(\text{CO})_3(\text{dmb})]$.

Contrary to the mechanism demonstrated herein, previous nanosecond⁴ and femto–picosecond⁵ time-resolved visible absorption spectra were interpreted assuming that the Re–Me homolysis is ultrafast, competitive with ISC to the $^3\text{MLCT}$ state.^{4,5} Moreover, it was concluded that $^3\text{MLCT}$ is an unreactive trapping state.^{4,5} This conclusion was based on the observation of two bands at 510 and 535 nm in the TR–vis spectra measured immediately after excitation. The 510 nm band, where the $[\text{Re}(\text{Solv})(\text{CO})_3(\text{dmb})]^*$ radical is known^{4,5} to absorb, does not change with time, while the 535 nm band, attributed to the $^3\text{MLCT}$ state, decays with a ~ 35 ns lifetime. In contrast, the present TRIR spectra clearly rule out any prompt Re–Me homolysis and prove that the reaction occurs from the $^3\text{MLCT}$ state. To reconcile these two sets of experiments, it is necessary to conclude that both bands at 535 and 510 nm seen in the earliest time-resolved visible spectra belong to the $^3\text{MLCT}$ state. The decay of the $^3\text{MLCT}$ state is, however, manifested only at 535 nm since the decay of the $^3\text{MLCT}$ absorption at 510 nm is compensated for by the concomitant rise of the radical absorption at the same wavelength. The existence of two maxima in the $^3\text{MLCT}$ spectrum is corroborated by the observation of two bands (475 and 510 nm) in the TR–vis spectra of $[\text{Re}(\text{Me})(\text{CO})_3(\text{dmb})]$ in a 2-MeTHF glass at 113 K, where the complex is photostable and only $^3\text{MLCT}$ is present.⁴ Results of previous

(48) Asbury, J. B.; Ghosh, H. N.; Yeston, J. S.; Bergman, R. G.; Lian, T. *Organometallics* **1998**, *17*, 3417–3419.

(49) Asbury, J. B.; Hang, K.; Yeston, J. S.; Cordaro, J. G.; Bergman, R. G.; Lian, T. *J. Am. Chem. Soc.* **2000**, *122*, 12870–12871.

(50) Dougherty, T. P.; Heilweil, E. J. *J. Chem. Phys.* **1994**, *100*, 4006–4009.

(51) Snee, P. T.; Payne, C. K.; Kotz, K. T.; Yang, H.; Harris, C. B. *J. Am. Chem. Soc.* **2001**, *123*, 2255–2264.

(52) Yang, H.; Snee, P. T.; Kotz, K. T.; Payne, C. K.; Harris, C. B. *J. Am. Chem. Soc.* **2001**, *123*, 4204–4210.

(53) Asplund, M. C.; Snee, P. T.; Yeston, J. S.; Wilkens, M. J.; Payne, C. K.; Yang, H.; Kotz, K. T.; Frei, H.; Bergman, R. G.; Harris, C. B. *J. Am. Chem. Soc.* **2002**, *124*, 10605–10612.

(54) Portius, P.; Yang, J.; Sun, X.-Z.; Grills, D. C.; Matousek, P.; Parker, A. W.; Towrie, M.; George, M. W. *J. Am. Chem. Soc.* **2004**, *126*, 10713–10720.

Table 1. $\nu(\text{CO})$ IR Wavenumbers of the Complexes, Excited States and Intermediates, and Photoproducts Studied Herein

species	solvent	$\nu(\text{CO})$ and label	figure
<i>fac</i> -[Re(Et)(CO) ₃ (dmb)]			
<i>fac</i> -[Re(Et)(CO) ₃ (dmb)]	MeCN	1987, 1867 (br)	2
<i>fac</i> -[Re(Et)(CO) ₃ (dmb)]	CH ₂ Cl ₂	1987, 1870 (br)	3
³ MLCT-[Re(Et)(CO) ₃ (dmb)]	MeCN	2015(A), 1926–1931(B), 1905(C)	2
³ MLCT-[Re(Et)(CO) ₃ (dmb)]	CH ₂ Cl ₂	2016(A), 1926(B), 1906(C)	3 bottom
[Re(MeCN)(CO) ₃ (dmb)]*	MeCN	2011(D), 1895–1900(E)	2
[Re(MeCN)(CO) ₃ (bpy)]* ^a	MeCN	2011, 1895 (br)	
#[Re(...MeCN)(CO) ₃ (dmb)]* ^b	MeCN	1960–1976(F), 1890–1895(E')	2
[Re(Cl)(CO) ₃ (dmb)]* ⁻	CH ₂ Cl ₂	1996(G), ~1891(H)	3
[Re(Cl)(CO) ₃ (dmb)]* ^{-c}	THF	1996, 1883, 1868	
[Re(CH ₂ Cl ₂)(CO) ₃ (dmb)]*	CH ₂ Cl ₂	2011(I)	3 top
[Re(Cl)(CO) ₃ (dmb)]*	CH ₂ Cl ₂	2020(J), ~1915(K)	3 top
[Re(CH ₂ Cl ₂)(CO) ₃ (dmb)] ⁺	CH ₂ Cl ₂	2034(L), ~1935(M)	3 top
<i>fac</i> -[Re(Me)(CO) ₃ (dmb)]			
<i>fac</i> -[Re(Me)(CO) ₃ (dmb)]	MeCN	1987, 1867	4
<i>fac</i> -[Re(Me)(CO) ₃ (dmb)]	CH ₂ Cl ₂	1989, 1872	5
³ MLCT-[Re(Me)(CO) ₃ (dmb)]	MeCN	2030(N), 1900–1960(O)	4
³ MLCT-[Re(Me)(CO) ₃ (dmb)]	CH ₂ Cl ₂	2028(N), 1910–1960(O)	5
[Re(MeCN)(CO) ₃ (dmb)]*	MeCN	2011(P), ~1900(Q)	4 middle, top
[Re(MeCN)(CO) ₃ (dmb)] ⁺	MeCN	2034(T), 1932(S)	4 top
[Re(CH ₂ Cl ₂)(CO) ₃ (dmb)]*	CH ₂ Cl ₂	2012(P), ~1902(Q)	5
[Re(CH ₂ Cl ₂)(CO) ₃ (dmb)] ⁺	CH ₂ Cl ₂	2034(R)	5

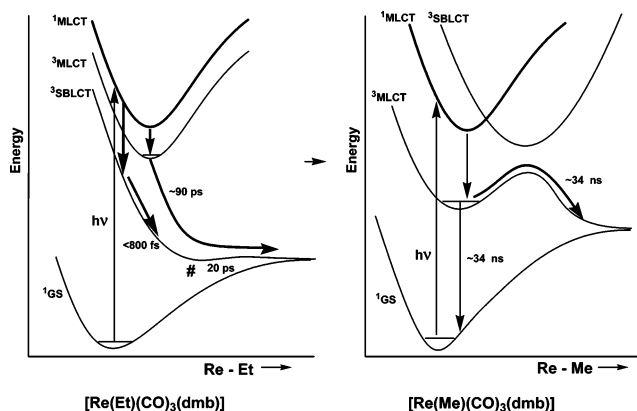
^a Electrochemically generated, from ref 43. ^b Tentative assignment, see text. ^c Electrochemically generated, from refs 43, 44.

nanosecond TRIR experiments⁴ also differ from those presented herein. The previous nanosecond spectra indicated that the radical formation is faster than the ³MLCT decay. However, these experiments used a different experimental setup employing 7 ns, 355 nm pulses, which were much stronger and longer (7 ns vs ~1 ns) than those used herein. The fast radical formation in those experiments apparently originated in multiple and two-photon excitations. This is independently demonstrated by quantum yield values estimated from the previously measured nanosecond TRIR spectra, being much larger than those determined under stationary irradiation⁴ and the picosecond TRIR reported herein. Photochemical reactions caused by multiple excitations were seen also in other studies performed with the same nanosecond TRIR experimental setup.⁵⁵

The different excited-state behavior of the ethyl and methyl complexes can be rationalized using qualitative potential energy curves of the relevant excited states along the Re–R reaction coordinate, Scheme 3. For [Re(Et)(CO)₃(dmb)], the dissociative ³SBLCT state is the lowest state at the geometry of the optical (i.e., vertical) excitation, as well as everywhere along the Re–Et coordinate. The optically populated ¹MLCT Franck–Condon excited state can undergo intersystem crossings to both the ³SBLCT and ³MLCT states. Population of the ³SBLCT state from the Franck–Condon state leads to prompt Re–Et homolysis. It is too fast, ca. ~800 fs,⁵ to dissipate the large energy excess to the solvent bath. Instead, the radical is formed vibrationally hot and equilibrates (cools) subsequently, with a 20 ps time constant. ³MLCT excited states of neutral Re carbonyl-polypyridine complexes typically live for tens of nanoseconds, decaying directly to the ground state.^{56–58} In [Re(Et)(CO)₃(dmb)], a reactive ³SBLCT state occurs between the ³MLCT state and the ground state. Instead of to the ground state, the ³MLCT state decays onto the dissociative ³SBLCT surface. Strong coupling and a small energy difference between the ³MLCT and ³SBLCT states make this conversion very fast, shortening the ³MLCT lifetime to about 90 ps. Regeneration of

the ground state is cut off. Thus, the photochemical quantum yield is unity² and the complex is not emissive, even in a 77 K glass.⁴ Earlier nanosecond and quantum yield studies have shown that this mechanism applies also to analogous complexes with isopropyl or benzyl ligands.^{2, 4}

Scheme 3. Qualitative Excited-State Potential Energy Curves along Re–R Coordinates and Excited-State Behavior of [Re(Et)(CO)₃(dmb)] (left) and [Re(Me)(CO)₃(dmb)] (right)^a



^a Based on quantum chemical calculations of model complexes.^{23,26,28,59,60} # denotes the vibrationally hot intermediate observed on the prompt pathway. Its actual position on the reaction coordinate and exact character are unknown. The position would shift from the left to the right for a hot ³SBLCT state, radical pair, and the hot radical #[Re(...MeCN)(CO)(dmb)]*, respectively.

The situation is profoundly different for [Re(Me)(CO)₃(dmb)]; see Scheme 3, right. The ³SBLCT state lies above the optically populated Franck–Condon ¹MLCT state at the geometry of the optical excitation, excluding the ¹MLCT → ³SBLCT intersystem crossing and, hence, the prompt homolysis pathway. Instead, the ³MLCT state is populated with a unit efficiency. The energy of the ³SBLCT state decreases sharply along the Re–Me coordinate, leading to a strongly avoided crossing with the

(55) Johnson, F. P. A.; George, M. W.; Turner, J. J. *Inorg. Chem.* **1993**, *32*, 4226–4229.

(56) Worl, L. A.; Duesing, R.; Chen, P.; Della Ciana, L.; Meyer, T. J. *J. Chem. Soc., Dalton Trans.* **1991**, 849–858.

(57) Kalyanasundaram, K. *J. Chem. Soc., Faraday Trans. 2* **1986**, *82*, 2401–2415.

(58) Blanco Rodríguez, A. M.; Gabrielsson, A.; Motevalli, M.; Matousek, P.; Towrie, M.; Šebera, J.; Zálíš, S.; Vlček, A., Jr., *J. Phys. Chem. A* **2005**, *109*, 5016–5025.

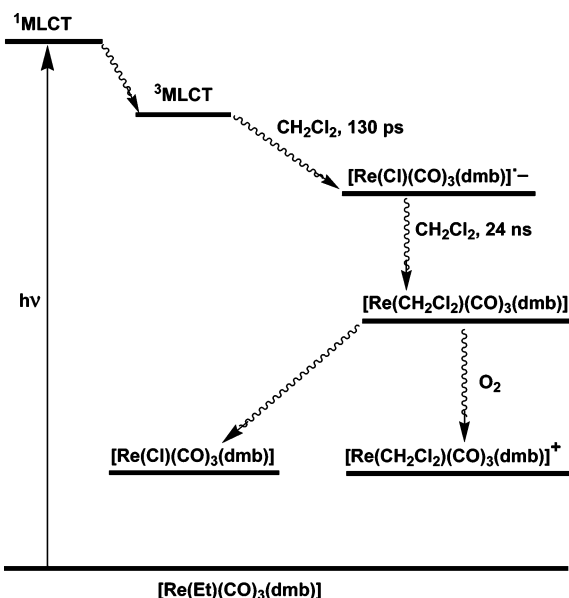
$^3\text{MLCT}$ state upon elongation of the Re–Me bond. A barrier arises on the $^3\text{MLCT}$ potential energy surface, which acquires partly $^3\text{SBLCT}$ character after the maximum.²⁶ The Re–Me homolysis can thus be viewed as an adiabatic evolution on an excited-state potential energy surface whose character gradually changes from $^3\text{MLCT}$ to $^3\text{SBLCT}$. Overcoming the barrier leads to the radical products. The relatively slow rate of the Re–Me homolysis allows for a simultaneous $^3\text{MLCT}$ decay to the ground state. At room temperature, the Re–Me homolysis and decay to the ground state have comparable time constants, ca. 34 ns. The homolysis slows down at lower temperatures, and the decay becomes prevalent.⁴

In summary, the remarkable differences between the mechanisms, yields, and rates of the Re–Et and Re–Me homolysis in $[\text{Re}(\text{R})(\text{CO})_3(\text{dmb})]$ originate in different relative energies of the Franck–Condon $^1\text{MLCT}$, dissociative $^3\text{SBLCT}$, and bound $^3\text{MLCT}$ excited states at the ground-state geometry and along the reaction coordinate. For $[\text{Re}(\text{Me})(\text{CO})_3(\text{dmb})]$, the $^3\text{SBLCT}$ state lies above both $^1\text{MLCT}$ and $^3\text{MLCT}$ states at the ground-state geometry and cannot be populated after optical excitation until it mixes (“crosses”) with the $^3\text{MLCT}$ state further along the reaction coordinate. Optical excitation is thus followed solely by intersystem crossing to the $^3\text{MLCT}$ state. A relatively slow, thermally activated Re–Me homolysis, which competes with the decay to the ground state, occurs from the $^3\text{MLCT}$ state. Changing the alkyl ligand from Me to Et stabilizes²⁷ the $^3\text{SBLCT}$ state, which becomes the lowest state everywhere along the reaction coordinate.⁵⁹ It is populated both from the Franck Condon $^1\text{MLCT}$ state and from the $^3\text{MLCT}$ state, resulting in the prompt and “delayed” Re–Et homolysis, respectively. $^3\text{MLCT}$ is no longer a “trapping” state, but an intermediate of the homolytic reaction. The decrease in the $^3\text{SBLCT}$ energy on going from Me to Et is caused by weakening the Re–C bond,^{27,61} which decreases the energy of the σ orbital, while the energies of the dmb-localized π^* orbital and Re d_π orbitals stay approximately constant. Consequently, the $^3\text{SBLCT}$ drops in energy relative to $^1,^3\text{MLCT}$ states when the Me ligand is replaced by Et. In addition, the smaller Re–Et than Re–Me dissociation energy pulls the whole $^3\text{SBLCT}$ potential energy surface lower, as is shown in Scheme 3.

It is interesting to note that these photochemical mechanisms cannot be understood from the knowledge of the excited states and the bonding and antibonding properties of the orbitals involved in the optical excitation at the ground-state geometry. Instead, it is necessary to consider the potential energy curves of all relevant excited states, their interactions, and character changes along relevant reactive and relaxation pathways.³⁰ This is well demonstrated by $[\text{Re}(\text{Me})(\text{CO})_3(\text{dmb})]$, whose $^3\text{MLCT}$ state becomes reactive only through interactions with higher excited states, later along the reaction coordinate.

Photochemistry in CH_2Cl_2 presents another intriguing problem. In earlier studies,^{2–4} it was assumed that the primary photochemical step, that is, the Re–R homolysis leading to the radicals, does not depend on the solvent. Herein, it is shown that this is the case only for the Me complex: The solvated radical $[\text{Re}(\text{Solv})(\text{CO})_3(\text{dmb})]^\bullet$ is formed from the $^3\text{MLCT}$ state of $[\text{Re}(\text{Me})(\text{CO})_3(\text{dmb})]$ with a time constant of ca. 34 ns both in MeCN and in CH_2Cl_2 . In the latter solvent, a much lower secondary abstraction of a Cl atom follows, producing $[\text{Re}(\text{Cl})(\text{CO})_3(\text{dmb})]$. In contrast, the $^3\text{MLCT}$ state of $[\text{Re}(\text{Et})(\text{CO})_3(\text{dmb})]$

Scheme 4. Photochemistry of $[\text{Re}(\text{Et})(\text{CO})_3(\text{dmb})]$ in CH_2Cl_2 ^a



^a The reaction products formed from CH_2Cl_2 and the ethyl group were not identified. The minor pathway involving the hot species F is not shown.

$[\text{Re}(\text{Et})(\text{CO})_3(\text{dmb})]$ reacts with CH_2Cl_2 to form $[\text{Re}(\text{Cl})(\text{CO})_3(\text{dmb})]^\bullet-$ with a time constant of ~ 130 ps. This reaction formally involves oxidation of the Et ligand in the excited complex by CH_2Cl_2 to “Et⁺”, and Cl^- coordination to the Re atom. It seems to be enabled by the SBLCT admixture to the $^3\text{MLCT}$ state, which leads to a partial Et⁺–Re^I bond character in the excited state. The complete absence of any features due to the radical $[\text{Re}(\text{CH}_2\text{Cl}_2)(\text{CO})_3(\text{dmb})]^\bullet$ in the TRIR spectra indicates that also the promptly formed $^3\text{SBLCT}$ state reacts preferentially with CH_2Cl_2 to $[\text{Re}(\text{Cl})(\text{CO})_3(\text{dmb})]^\bullet-$, preventing any formation of the radicals. The excited state of $[\text{Re}(\text{Me})(\text{CO})_3(\text{dmb})]$ is unreactive toward CH_2Cl_2 probably because of its purer $^3\text{MLCT}$ character and greater stability of the Re–Me bond.

Conclusions

Both $[\text{Re}(\text{R})(\text{CO})_3(\text{dmb})]$ complexes (R = Me, Et) in CH_3CN undergo photochemical Re–R bond homolysis producing the radicals $[\text{Re}(\text{Solv})(\text{CO})_3(\text{dmb})]^\bullet$ and R[•].

The Re–Et homolysis occurs by two parallel pathways: prompt (~ 800 fs) and delayed (~ 90 ps). Optical excitation of $[\text{Re}(\text{Et})(\text{CO})_3(\text{dmb})]$ populates a $^1\text{MLCT}$ state, which undergoes two parallel subpicosecond intersystem crossings to a dissociative $^3\text{SBLCT}$ state and a bound $^3\text{MLCT}$ state. Population of $^3\text{SBLCT}$ leads to a subpicosecond (~ 800 fs) formation of vibrationally and solvationally unequilibrated (hot) radicals. Their relaxation/solvation to $[\text{Re}(\text{CH}_3\text{CN})(\text{CO})_3(\text{dmb})]^\bullet$ occurs with 20 ps kinetics. The $^3\text{MLCT}$ state also converts to the reactive $^3\text{SBLCT}$ state, but with a slower rate, ~ 90 ps, ultimately also resulting in radical formation.

The Re–Me homolysis is much slower. It occurs from the relaxed $^3\text{MLCT}$ state only. The optically populated $^1\text{MLCT}$ excited state of $[\text{Re}(\text{Et})(\text{CO})_3(\text{dmb})]$ undergoes subpicosecond intersystem crossing to a $^3\text{MLCT}$ state, which decays to the ground state and, in parallel, undergoes a thermally activated Re–Me homolysis. Both reactions occur with approximately the same time constant (~ 34 ns) at room temperature. The photochemical quantum yield is determined on a nanosecond time scale by the branching of the $^3\text{MLCT}$ excited-state

(59) Guillaumont, D.; Finger, K.; Hachey, M. R.; Daniel, C. *Coord. Chem. Rev.* **1998**, *171*, 439–459.

(60) Daniel, C. *Coord. Chem. Rev.* **2003**, *238–239*, 143–166.

(61) Siegbahn, P. E. M. *J. Phys. Chem.* **1995**, *99*, 12723–12729.

evolution between the reaction and relaxation to the ground state. This is documented by the close similarity of the quantum yields determined by TRIR and stationary irradiation.

The different excited-state behavior of both complexes is caused by different relative energies of the Franck–Condon 1 -MLCT, reactive 3 SBLCT, and “trapping” 3 MLCT excited states at the ground-state geometry and along the Re–R reaction coordinate. In the case of the ethyl complex, 3 SBLCT is the lowest state everywhere along the reaction coordinate. For the methyl complex, it lies above both the singlet and triplet MLCT states and becomes lower in energy only upon elongation of the Re–R bond.

$[\text{Re}(\text{Solv})(\text{CO})_3(\text{dmb})]^*$ radicals are rather stable in MeCN. They undergo slow (μs) secondary thermal reactions with CH_2Cl_2 or air, producing $[\text{Re}(\text{Cl})(\text{CO})_3(\text{dmb})]$ or $[\text{Re}(\text{Solv})(\text{CO})_3(\text{dmb})]^+$, respectively.

The 3 MLCT excited state of $[\text{Re}(\text{Et})(\text{CO})_3(\text{dmb})]$, but not of its Me counterpart, reacts with CH_2Cl_2 to form $[\text{Re}(\text{Cl})(\text{CO})_3(\text{dmb})]^*$. The difference in reactivity is caused by slightly different excited-state characters of the Et and Me complexes and Re–R bond energies.

It follows that interpretation and prediction of organometallic photochemistry requires understanding of the energetics and characters of electronic excited states not only at the ground-state geometry, where the optical excitation occurs, but also along all relevant reaction and relaxation coordinates. Photochemical metal ligand bond-homolysis clearly occurs from triplet states, 3 SBLCT or 3 MLCT. This reactivity contrasts photochemical M–CO dissociation, which is a femtosecond spin-singlet process, with 3 MLCT states behaving as unreactive traps.^{30,62–64}

Acknowledgment. This research was funded by EPSRC, CCLRC, Queen Mary, University of London, and by the European COST D14 collaboration program.

OM0508886

(62) Farrell, I. R.; Matousek, P.; Towrie, M.; Parker, A. W.; Grills, D. C.; George, M. W.; Vlček, A., Jr. *Inorg. Chem.* **2002**, *17*, 4318–4323.

(63) Vichová, J.; Hartl, F.; Vlček, A., Jr. *J. Am. Chem. Soc.* **1992**, *114*, 10903–10910.

(64) Vlček, A. J. *Coord. Chem. Rev.* **2002**, *230*, 225–242.